SHINE 2005, Kona, Hawaii

Poster Preview

POSTER SESSIONS (with refreshments):

Monday, Tuesday and Thursday 5:00 ~7:00

1. Campaign Events: 5 Posters
2. Working Group 1: Solar 55 Posters
3. Working Group 2: Interplanetary 33 Posters
4. Working Group 3: Energetic Particles 17 Posters

Campaign Events:

Apr 7, and May 12, 1997

Coronal Magnetic Field and IMF Structure:

Titov et al. – Analytical model of May 12 - large scale background field + localized dipole (AR) → union of 2 intersecting quasi-separatrix layers.

**33 Ledvina et al.* - ZEUS-3D MHD model of solar corona; open/closed field configurations around event sites. (1997 + Halloween).

Arge et al. -High resolution remapped Mt. Wilson magnetograms as input to Wang-Sheeley-Arge model to get coronal magnetic field, solar wind speed and IMF polarity at 1 AU.

Bharti et al. – Qualitative model to interpret multispectral observations. Flux cancellation → blast wave producing a CME and C-class X-ray flare with at least two phases of energy release.

April 21, and Aug 24, 2002:

Komm et al. - Sub-surface evolution; determine flows down to depths of 16 Mm and flow history prior to April and Aug events. Systematic variation in kinetic helicity density → subsurface indicator of flare?

Halloween Events 2003:

Cohen et al. - Heavy Ion spectra and composition: Event-integrated composition varies between events and depends heavily on energy within an SEP event.

**15 Daou and Alexander* – Hard X-ray substructure (RHESSI) improves understanding of strength and distribution of energy deposition in flares.

**98 Evenson et al.* - Attempt to identify the source region of energetic radiation by comparing emission time structure of neutrons and gamma rays with optical data and injection profile of GeV protons.

**74 Kuwabara et al.* –Geometry of ICME and shock deduced from network observations of cosmic ray anisotropy

Working Group 1: Solar

Theory / Models: Solar Structures

#6 Abbett – 3d MHD Simulations of Magnetic Flux Emergence in Active Regions – address inherent stiffness of system of equations.

#9 Barnes et al. Can Force-Free Extrapolations Reproduce the Coronal Magnetic Topology? Compare X-type separator (reconnection site) and separatrix surface with 'bald patch' may be kink unstable. Judge performance of linear and non-linear extrapolations.

Theory / Models: Ambient Solar Structures

#23. Gilbert et al. – New Technique for Mapping Open magnetic Flux from Sun to Heliosphere. Gives uniform distribution of flux in outer corona using a relaxation technique applied to the open flux to distribute it evenly across a surface of constant magnetic pressure.

#37 Lionello et al. An MHD Model of Differential Rotation We have imposed a magnetic flux distribution as in Fisk et al. (1999) Relax system to steady state and apply differential rotation.Changes are described.

#42. McGregor et al. Effects of Photospheric Field Processng on Derived Coronal Magnetic Field and HCS. Assess differences between coronal field models by first identifying effects from different treatments of BCs.

Theory / Models: Ambient Solar Structures

#44. McTiernan – Effect of Magnetogram Noise on Non-Linear Force Free Field Extrapolation. Discuss effects of randomly generated noise on field extrapolations. Results compared with 'true' field.

#52. Schuck – Accurate and Precise Estimation of Velocities and Uncertainties in Magnetograms. Local Correlation Tracking is inconsistent with magnetic induction equation. Present new technique that incorporates magnetic induction equation.

Theory / Models: Ambient Solar Structures

#26. Hanasoge et al. – Simulations of Acoustic Flow Interaction in Spherical Geometry – Simulate acoustic wave interaction with flows in spherical geometry – use results for validation of helioseismology.

#24. Green - Solar Supergranulation as Propagating Waves: Phase speeds are found to be greater than the surface speed, possibly explaining observations that SG pattern appears to rotate faster than photospheric plasma

#35. Green – Supergranulation Waves in Sub-surface Shear Layer. Rotation difference between supergranulation and photosphere may bbe due to instabilities in convective shear layer.

Theory / Models: Ambient Solar Structures

#41. Magara et al. MHD Simulation of Magnetic U-Loops and Flux Cancellation on the Sun.
Simulate flux cancellation through the emergence of U-shaped field lines.

Observations: Ambient Solar Structures

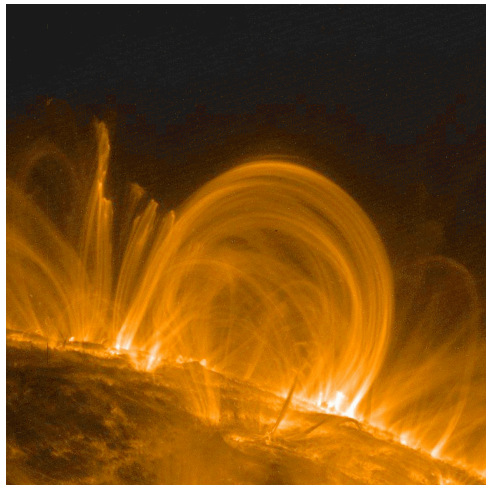

#10 Brosius and White: **Coronal Magnetic Field Measurements Above a Sunspot (VLA). Derive, unambiguously, the height dependence of magnetic field.**

#30. Jensen et al. The Cassini Faraday Rotation Experiment. Present observations of Faraday rotation due to product of electron density and parallel magnetic field for 2002 coronal magnetic field

#55Tomczyk – Initial magnetic Field Measurements from the Coronal Multi-Channel Polarimeter (COMP).Initial measurements of coronal field are presented and methodology is described.

Observations: Solar Structures

#34. Leka and Metcalf - Chromospheric Magnetic Field Observations and Solar Energetic Events. Present measurements of chromospheric field observations which should provide direct insights into energy storage for solar energetic events.

***#32 Komm et al.* - Sub-surface Flows near AR. ARs show convergent horizontal flows, implying downflows at depths less than 10Mm and divergent flows at greater depth, implying upflows.**

#16 de Toma et al. Coronal Holes in Cycle 23. Discuss identification method, changes in area, latitudinal distributions, and maximum vs. minimum phase including time of polar reversal.

Observations: Solar Structures

#12 Butala – Reconstruction of Coronal Electron Density using solar rotational tomography from white light polarized brightness.

#28 Jensen et al. – Cassini Measurement of Coronal Electron Density. Find Tyler et al. (1979) model gives best fit to background field.

#51. Sandman et al. 3D Visualizations of Solar Corona: Applications and Results. Builds on photospheric magnetic field models of Schrijver and DeRosa (2003) and Schrijver and Aschwanden(2002). Simulations are used to develop reconstruction tools for STEREO

Observations:Solar

#45. Minarovjech and Rusin: Comparison of variation of solar indices and cosmic ray neutron monitor intensities. Investigation covers period from 1986 to 2005.

Theory and Models: CMEs

 # 13. *Chane et al.*- CME 'seismology'?
Numerically simulate evolution of CMEs from Sun to 1 AU with 2.5D (axisymmetric) ideal MHD model using info at 1AU (reverse-engineering).

#17 *DeVore and Antiochos* – Magnetic Free Energies of Breakout CMEs (episode 2). Pre-opening highest field lines lowers threshold free energies for CME onset. Available CME energies higher for 'side' arcades. Simultaneous eruptions not expected to occur.

#40. Lynch et al. First Demonstration of 3D Breakout. Present numerical results with NRL 3D sperical ARMS code. Breakout produces fast >2000k/s CMEs and classic flare reconnection beneath expanding inner arcade.

Theory and Models: CMEs

#21. *Gibson et al.* – End-states of erupting and partially erupting magnetic flux ropes. 3-D MHD simulations capture observed properties of coronal post-CME state. Also discuss how the pre-event coronal state affects the ultimate post-CME state of corona.

#22 Jacobs et al. Quantification of CME triggering mechanisms. Ideal MHD simulations using finite volume, explicit solver. Two triggers: foot point shearing and flux emergence.

***33 Ledvina et al. -* ZEUS-3D MHD model of solar corona; open/closed field configurations around event sites. (1997 + Halloween).**

Theory and Models: CMEs

#19 *Forbes and Isenberg* – Equilibrium and Evolution in 3D Flux Rope CME. Analytic; incorporates full effect of line-tying. Explains failure of some erupting flux ropes to escape, strong out-of-plane twisting and more!

#36. Lin -Nature of Reconnecting Current Sheet by CME/Flare – Results indicate that values of diffusivity deduced for 3 events are all 10-12 and 6-8 orders of magnitude greater than those of classical and anomalous diffusivities respectively

#49. Reeves – Light Curves for Loss of Equilibrium Model of Solar Eruptions. Use model to determine the thermal energy release by assuming that all of the Poynting flux flowing into reconnection region is thermalized.

Theory and Models: CMEs

#50. Riley et al. Bursty Reconnection during Solar Eruptions: MHD Simulations and Comparison to Observ. Focus on the formation and evolution of 'blobs' within the reconnection site and compare to LASCO observations.

#57 Wu et al. Numerical MHD Simulation of Key Parameters for CME Initiation – Model is used to simulate the CME production parameters of Falconer et al. (2002) and shows good agreement with observations.

#60. Zhao – Ice-Cream Cone Model for Halo CMEs. We improve our cone model to determine the geometrical and kinematical properties of halo CMEs. In two cases shown, these properties can be uniquely determined.

Observations: CMEs

#7. Akiyama et al. CME-rich and –poor Active Regions. Not all active regions are created equal. Some are extremely productive – differences will be discussed.

#11 Burkepile et al. CMEs in the Low Corona. Acceleration peaks, widths speeds are lower. SEP events associated with west-limb CMEs that are very fast and wide in low corona.

#47. Nitta and Burkepile – Revisiting relation between CMEs and flare-associated ejections. Use low corona observations to get better timing on formation of CMEs to compare with SXT high-time cadence data.

Observations: CMEs

#20. *Georgoulis and LaBonte* –Real-Time Prediction of Eruption Potential in AR: Compute magnetic energy and helicity using vector magnetic field data. There is a clear distinction in the total helicity and non-potential energy between eruptive and non-eruptive ARs.

#18. Falconer – Forecasting CMEs from LOS magnetograms. 2 improved measures using total length of strong-field neutral line: shear weighted and magnetic-gradient weighted. Both have 75% success rate.

***#22. Gilbert* – Application of new technique for deriving prominence mass from EIT FeXII absorption features. Accurate determinations of mass may help assess the dynamical importance of prominences in CMEs.**

Observations: CMEs

#43. Michalek et al. Geoeffectiveness of halo CMEs. Show that major geomagnetic storms are caused by very fast halo CMEs originating from western hemisphere close to central meridian. Strength of storm does not depend on width.

#58. Yashiro et al. Visibility of CMEs as a function of X-ray flare location and intensity. All fast and wide CMEs are detectable by LASCO but slow and narrow near disk center may not be visible.

#48 Qiu – Role of Magnetic Reconnection in Early-stage Mass Ejection. Examine reconnection-acceleration relationship in events with different magnetic configurations (bi-polar vs. multi-polar).

Observations: CMEs

#53. Starr et al. Celebration of 40 Years of Mauna Loa Solar Observatory. MLSO data used to study CMEs, promience eruptions, waves, transient coronal holes, are pre- and post-event corona.

#54. Tian et al. Helicity injection associated with sigmoid eruptions an onset of powerful CMEs. Study helicity injection for two events (Nov 2001) with large flares, strong proton events and very fast CMEs. Results provide clues to role of helicity in eruptions.

#56. Welsch and Li – Active Region Flows and Eruptive Events – Use LCT and feature tracking (FT) to determine baseline flow speeds and relationship

Observations: CMEs

#59. Zhang – Observational Study of Velocity and Acceleration of CMEs. Find that CME velocity in the outer corona is determined by two factors, acceleration duration and acceleration magnitude. Slow CMEs are likely associated with solar wind dragging.

Observations / Models: CMEs

#29 Jensen and Russell – Modeling CME effects of Faraday Rotation – Observed rotation in plane of polarization. Compare events to modeled CME transients with respect to expansion velocity, clock and cone angles and maximum spiral pitch angle.

#35. Li and Luhmann, Coronal Magnetic Toploogy above CME source regions with filament eruptions. Use observations and PFSS model to investigate magnetic field configurations and topology around CMEs, in particular compare breakout and flux cancellation models

#39 Liu et al. Energy budget of Halo CMEs-related ARs Explore correlation between free energy in AR and energetics of corresponding CMEs

Observations: Flares

#14. *Coyner and Alexander* - UV and Hard X_ray evidence for 3D reconnection in Large Flares. Interaction of multi-flux systems.

***15 Daou and Alexander* – Hard X-ray substructure (RHESSI) improves understanding of strength and distribution of energy deposition in flares.**

***#27 – Hori et al*. – RHESSI and NoRH Observations of July 3, 2002 Flare. Magnetic flux emergence heavily distorted shape of neutral line where X1.5 flare occurred. Event was not eruptive – suggesting most of released energy was confined to flare region.**

Observations: Flares

#38 Liu and Alexander: Characteristics of Hard X-ray Production in Flares Driven by Filament Eruptions. Compare 'successful' and 'failed' eruptions. Event failed eruptions can generate significant energy release and hard X-rays.

#39 Nightingale et al. TRACE observations of X-flares and Rotating Sunspots. All observed X-class flares are associated with 23 AR containing 46 rotating sunspots which appear to be manifestations of twist and/or writhe

Working Group 2: Interplanetary

Observations

#61 Watanachak and Zhang: Identification of Solar Source Regions of 79 major storms from 1996-2004. 82% are caused by front-side halo CMEs, 15% by CIRs related to coronal holes on disk and 3% are unidentified.

#62. Rodriguez et al. A Study of Drift Rates of Type II bursts ad Different Wavelengths. Find drift rate can be approximated by a power law. Discuss implications of frequency dependence of drift rate in terms of evolution of associated CME.

Observations – Interplanetary

#63 Chen et al. Mechanism for irreversible dissipation at collisionless shocks: Nonlinear ion acoustic instability. Cassini observations of electrostatic waves at bow shocks of saturn and earth suggest the dominant wave component at both bow shocks to be nonlinear ion acoustic waves.

#66 Gopalswamy et al. CME Kinetic Energy and the Wavelength Range of Type II Bursts. We find that the CME kinetic energy seems to organize the lifetime of the type II bursts. Contrary to previous results, the starting frequency of metric type IIs with IP counterparts is no different from those without IP counterparts.

Observations – Interplanetary

#68. Jackson et al. -Interactive Visualization of Solar Mass Ejection Imager (SMEI) and IPS Volumetric Data. We present a volume rendering system developed for real-time visualization and manipulation of 3D Heliospheric volumetric solar wind density and velocity.

#69. Jian et al. Identifying and Distinguishing ICMEs from Stream Interaction Regions (SIRs). Method needed to distinguish these. We use requirement that ICME pressure should reach at least 40 pPa, velocity change should be at least 30 k/s and there should be evidence of magnetic structure.

Observations – Interplanetary

#70. Jian et al. Solar Cycle Variation of the Properties of Streamer Interaction Regions (SIRs). We find that the occurrence rate of shocks at SIRs is about 30% on avg. and declines during rise of solar cycle, while number of SIRs shows little variation. Also find that field rotations occur at sector boundaries ahead of SIRs.

#71 Kataoka et al. Downstream structures of IP fast shocks associated with CMEs. Focus on fine structures in the sheath region between CME and shock. Characteristics depend on the shock angle to the flow, and the Alfven Mach number.

Observations – Interplanetary

#72 Korreck et al. – Heating of Heavy Ions by CME-driven Collisionless Shocks. Study focuses on thermal velocities from ACE for 19 shocks. Heating found to be dependant on plasma and shock magnetic angle.

#73 Krall et al. Flux-Rope CME Geometry and its Relation to Observed CME Morphology. Use a simple parameterization of 3D flux rope to determine typical flux-rope geometry to produce statistical measures of morphology for comparison with statistical measures of observed CME flux-rope morphology.

Observations – Interplanetary

#74. Kuwabara et al. Geometry of ICME and shock deduced from network observations of cosmic ray anisotropy. We suggest that the 'loss-cone' anisotropy in the event of Oct 29, 2003 has a rather broad pitch-angle distribution about the IMF implying the shock is 'quasi-parallel'

#75 Lal - Geomagnetic Storm Induced Gravity Waves. Study of the influence of geomagnetic storm at low latitudes in the northern hemisphere. There is enhancement in the amplitude of the acoustic gravity waves obtained immediately after severe storms. Detailed results are presented.

Observations – Interplanetary

#76. Lopez-Portela, IP Magnetic Clouds and Their Geoeffectiveness. Main objective is to study MCs with and without sheaths to determine if those with sheath regions are more geoeffective.

#78 Mays et al. Can We Detect CMEs in Lyman-alpha?We report a negative detection for the 4 best candidate events.

#79 Luo et al. Correlation between the Magnetic Fields Measured by ACE and WIND. Due to the appropriate separation between the spacecrafts, the measured magnetic fields exhibit a high degree of coherence.

Observations – Interplanetary

#80. Moise et al. How significant is electron impact ionization in producing He+ Pick-up Ions (PUI) at and within 1 AU. We explore the relative importance of electron-impact ionization of interstellar He.

#83. Pagel et al. Scattering of suprathermal electrons in the solar wind. Focus on a subset of strahl broadening events, when dlBl/lBl is high, we find a characteristic energy dependence of strahl scattering which may be explained by resonance with whistler waves.

#85. Reinard – Comparison between coronal dimming regions and CMEs. We determine the relative dimming and compare to CME mass as determined by LASCO.

Observations – Interplanetary

#84. Petty et al. CME Characteristics of Decametric-Hectometric (DH) Type IV Radio Bursts by Wind/WAVES. Results suggest that DH type IVs are continuations of metric events, indicating broader frequency type IV bursts are created by faster CMEs.

#86. Richardson and Cane – Survey of ICMEs in the Near-Earth Solar Wind During 1996-2005. Extend our comprehensive survey to include the declining phase of cycle 23. We discuss variation in properties, the fraction of ICMEs that are magnetic clouds and the relation between ICME and CME properties, and geomagnetic storms.

Observations – Interplanetary

#88. Russell et al. Solar Cycle Variation of the Properties of ICMEs. We have used the total perpendicular pressure to identify and characterize ICMEs. We give the occurrence rate, peak pressure and maximum magnetic field of three groups of ICMEs based on 9 years of WIND data.

#89 Sterling et al. Streamer Puffs from Homologous Compact Ejective Flares. We take our eruptions to be a new variety of narrow CME, which we call streamer puffs.

#93. Xie et al. Fe Charge States in and Outside Magnetic Clouds. Results show that the enhancement is only present in the Magnetic cloud and not the sheath region.

Observations – Interplanetary

#90 Velli et al. **Origin of Heliospheric Magnetic Field Polarity Inversion at High Latitudes.** We suggest the cases of reversal of radial magnetic field polarity observed by Ulysses are due to the coupling of standard large amplitude Alfvenic turbulence in the low frequency regime propagating away from the sun.

#92. Viall et al. **Exploring the Occurrence Rate of Solar Wind Periodic Number Density Structures.** Present statistical examination of the periodic number density structures in the solar wind in order to establish the occurrence frequency of significant spectral peaks.

Theory / Models - Interplanetary

#64. Cohen et al. Transport of the Solar Open Flux with Spatial Diffusion – 2D Simulation.We present a 2D numerical simulation of the Fisk diffusion model on the surface of the sun.

#77. Lugaz and Manchester - 3D Simulation of the interaction of two CMEs from Sun to Earth. Use a 3D compressible MHD model. At Earth the two magnetic clouds can still be distinguished with a compressed and heated first cloud and a second over-expanded cloud.

Theory / Models - Interplanetary

#81. Owens et al. - An improved Flux-Rope Model of Magnetic Clouds (MC). We attempt to make non-circular cross-section fits but to constrain the additional fit parameters using ICME/CME observations and knowledge of physical processes acting on the MC.

#87. Ruffolo et al. Turbulence, dropouts and suppression of the field line random walk. We provide evidence that strong 2D turbulence can inhibit diffusion due to the slab component. Therefore, there can be sharp trapping boundaries where the 2D field is strongest.

Theory / Models - Interplanetary

#65. Farahat and Sabah – New Model for Proton Particles Interplanetary Propagation. The scattering of decayed protons along IP magnetic field lines is simulated and the measured proton flux is calculated. New model distinguishes between subatomic particles produced by direct decay of neutron solar flares and those produced in corona.

#66 Goodrich – Modeling the Solar-Terrestrial Environment as a Comprehensive System

Working Group 3: Energetic Particles

#94. Al-Dayeh et al. Elemental abundance variations of SEPs at low energies by Wind/STEP over the last solar cycle. We discuss the results of our measurements of the ratios of He/O, C/O, NeS/O and Fe/O at low energies over the most recent solar cycle.

#95. Al-Sawad et al. A Statistical study of High Energetic (~90 MeV) Proton Events observed with SOHO/ERNE during cycle 23. We find that most of those events are due to CMEs and many of these were associated with high intensity solar flares (X- and M-class)

Observations – Energetic Particles

#97. deKoning et al. Energy Dependent Broadening of Low-Energy Solar Electron Bursts. We present a study of suprathermal electron-pitch angle distributions observed in 2002 by ACE before, during and after solar bursts.

#98 Evenson et al. - Attempt to identify the source region of energetic radiation by comparing emission time structure of neutrons and gamma rays with optical data and injection profile of GeV protons.

#99. Haggerty and Roelof – Solar Proton and Near-Relativistic Electron Events – What is the Relationship? This study intends to answer very specific questions regarding near-relativistic electrons and energetic protons.

Observations – Energetic Particles

#102 Leske et al. Extending Measurements of Ultra-Heavy Elements in SEP events at Higher Energies. Among the results presented, we find that at these high energies even large gradual events are often very iron rich and may appear similar in composition to impulsive events.

#107. Ruffolo et al. Relativistic Solar Protons on 1989 Oct 22: Injection Along Both Legs of a Loop. We present results that suggest a model with simultaneous injection along both legs of a closed loop provides the best explanation to the observations.

Observations – Energetic Particles

#108. Spence et al. Comparison of SEP Events and Impulsive Nitrate Increases in Artic Ice Cores. We report on the correlation between impulsive nitrate spikes in ice strata and SEP events over past ~75 years.

#110 Wang et al. A Study of the Solar Injection for 11 Impulsive Electron/3He-rich SEP events. We are able to obtain the electron injection profile versus energy from the in-situ observations for all selected events and the ion injection profile for 1 event with good ion statistics.

Theory / Model – Energetic Particles

#96. Bieber et al. Record-Setting Ground Level Enhancement: Jan 20, 2005. We use data from 'Spaceship Earth' to model the time evolution of cosmic ray density and anisotropy to explain the observed increase by a factor of 30 by a neutron monitor at McMurdo, Antarctica.

#100 Hesse et al. Particle-in-cell Modeling of Electron Acceleration in Fast Shocks.We present the results of a fully-electromagnetic, relativistic, particle-in-cell simulations of fast shock structure and evolution.

Theory / Model – Energetic Particles

#103 Luhmann et al. **Macroscopic source and transport aspects of SEP event time profiles.** We utilize an improved global model of IP shocks developed by CISM to investigate the transport of ions in the >10 MeV range with the goal of sorting out the complicated origins of SEP event profiles.

#106. Qin et al. **The Effects of Adiabatic Cooling on the Rigidity Dependent SEP Mean Free Path.** We discuss the influence of adiabatic cooling effects on the rigidity dependence of mean free path in large gradual SEP events.

Model / Observations– Energetic Particles

#101. Krauss-Varban et al. ESP Events: Comparison Between ACE Observations and Simulations. We concentrate on ACE particle events with relatively mild Mach numbers (2 to 5) and study the energy range up to ~1MeV in order to help constrain models.

#105. Mulligan et al. GCR short-period variations and magnetic field modeling: Implications for ICME local and non-local geometries. Modeling of observations reveal that differences in decrease and recovery rates for MC topologies are due to non-local 3D characteristics of ICME shock, sheath and envelope regions.

Model / Observations– Energetic Particles

#109. Tylka et al. A Model for SEP Spectral and Compositional Variability at High Energies. We present results from a simple analytic model of shock accelerated SEP events which suggest the observed variability in observations is a natural consequence of the evolution of the shock normal angle, coupled with a compound seed population.

New Missions: Solar

#8 *Alexander et al*.- Solar Polar Imager → at 0.48 AU, inclination of 75°; observe AR longer.

New Missions: Interplanetary

#82. Oberoi et al. Solar and Heliospheric Applications of Low Frequency Radio Arrays. Remote sensing techniques using widefield radio arrays at low frequencies offer great promise in determining interplanetary densities, velocities, and magnetic fields from near sun to 1 AU. We discuss the design and status of the Mileura Widefield Array, Low Frequency Demonstrator.

New Programs

#91 Webb et al. The International Heliophysical Year (IHY) – An international program of scientific research. The IHY commemorates the 50th anniversary of the IGY and will focus on cross-disciplinary physics governing all heliophysics through the study of Universal Processes and Coordinated Campaigns.

New Missions– Energetic Particles

#104 Mukherjee – Neutral-atom physics in the Heliosphere. We present a neutral-atom instrument design for Solar Probe that uses Microelectromechanical (MEMs) devices massing only a few grams.